Supporting Information

Simulating Structural and Thermodynamic Properties of Carcinogen-Damaged DNA

Shixiang Yan,[*] Min Wu,[*] Dinshaw J. Patel,[†] Nicholas E. Geacintov,[*] and Suse Broyde[‡]

[*] *Department of Chemistry, New York University, New York, NY 10003, USA*

[†] *Cellular Biochemistry & Biophysics Program, Memorial Sloan-Kettering Cancer Center, New York, NY 10021, USA*

[‡] *Department of Biology, New York University, New York, NY 10003, USA*

Running Title: BP-dG DNA Structures and Thermodynamics

Abbreviations: (+)-*anti*-BPDE, (+)-(7*R*,8*S*,9*S*,10*R*)-7,8-dihydroxy-9,10-epoxy-7,8,9,10-tetrahydrobenzo[*a*]pyrene; (−)-*anti*-BPDE, (−)-(7*S*,8*R*,9*R*,10*S*)-7,8-dihydroxy-9,10-epoxy-7,8,9,10-tetrahydrobenzo[*a*]pyrene; BP, benzo[*a*]pyrene; BPDE, benzo[*a*]pyrene diol epoxide; DNA, deoxyribonucleic acid; MD, molecular dynamics; MM-PBSA, molecular mechanics Poisson–Boltzmann surface area; NER, nucleotide excision repair; NMR, nuclear magnetic resonance; NOE, nuclear Overhauser effect; PAH, polycyclic aromatic hydrocarbon; PME, particle mesh Ewald; RESP, restrained electrostatic potential fitting; RMSD, root-mean-square deviation; SASA, solvent-accessible surface area;

Keywords: benzo[*a*]pyrene diol epoxide DNA adduct structure and stability; molecular dynamics; free energy calculations; nucleotide excision repair; hydration

Address reprint requests to Suse Broyde, Department of Biology, New York University, New York, NY 10003, Telephone: 212-998-8231, Fax: 212-995-4015, Email: broyde@nyu.edu; and to Nicholas E. Geacintov, Department of Chemistry, New York University, New York, NY 10003, Telephone: 212-998-8407, Fax: 212-998-8421, Email: ng1@nyu.edu.

Table S1: Partial Charges, Atom Types and Topologies of 10*S* (+)- and 10*R* (−)-*trans-anti*-[BP]-N^2-dG Nucleotides

			Partial Charge	
Atom Name	Atom Type	Topology	10*S* (+)-*trans-anti*-[BP]-N^2-dG	10*R* (−)-*trans-anti*-[BP]-N^2-dG
P	P	M	1.17223	1.17028
O1P	O2	E	−0.77241	−0.77354
O2P	O2	E	−0.77241	−0.77354
O5'	OS	M	−0.49304	−0.49376
C5'	CT	M	−0.00687	−0.00688
H5'1	H1	E	0.07581	0.07568
H5'2	H1	E	0.07581	0.07568
C4'	CT	M	0.16379	0.16351
H4'	H1	E	0.11824	0.11804
O4'	OS	S	−0.39272	−0.39160
C1'	CT	B	0.04836	0.05561
H1'	H2	E	0.17746	0.15598
N9	N*	B	0.07581	0.10680
C8	CK	S	0.15343	0.11613
H8	H5	E	0.19888	0.20737
C4	CB	S	−0.01990	0.03152
C5	CB	B	0.33149	0.30313
N7	NB	E	−0.64661	−0.64696
C6	C	B	0.39564	0.45951
O6	O	E	−0.53584	−0.55905
N1	NA	B	−0.23906	−0.33858
H1	H	E	0.25981	0.30383
C2	CA	B	0.23568	0.30464
N3	NC	E	−0.27100	−0.38233
N	N2	B	−0.35480	−0.38592
HN	H	E	0.30405	0.32591
CC10	CT	B	−0.03026	−0.12798
HC10	H1	E	0.14237	0.18770
CC9	CT	3	0.25759	0.00281
HC9	H1	E	0.09371	0.18188
O9	OH	S	−0.63039	−0.59941
HO9	HO	E	0.38659	0.38323
CC8	CT	3	0.05912	0.25224
HC8	H1	E	0.14800	0.10931
O8	OH	S	−0.65885	−0.68483
HO8	HO	E	0.43345	0.42709
CC7	CT	3	0.13272	0.22805
HC7	H1	E	0.07420	0.02831
O7	OH	S	−0.64502	−0.64088
HO7	HO	E	0.44008	0.41133
C61	CA	S	−0.01781	−0.03409
CC6	CA	B	−0.15914	−0.15798
HC6	HA	E	0.17977	0.15869
C51	CA	B	−0.00498	−0.00060
C123	CA	E	0.02634	0.01365
CC5	CA	B	−0.15526	−0.14612
HC5	HA	E	0.14820	0.15146

Table S1: *Continued*

			Partial Charge	
Atom Name	Atom Type	Topology	10*S* (+)-*trans-anti*-[BP]-N^2-dG	10*R* (−)-*trans-anti*-[BP]-N^2-dG
CC4	CA	B	−0.18860	−0.19416
HC4	HA	E	0.15665	0.15739
C31	CA	B	0.06103	0.04647
C122	CA	E	0.09924	0.09345
CC3	CA	B	−0.18969	−0.15628
HC3	HA	E	0.16369	0.16000
CC2	CA	B	−0.19218	−0.20791
HC2	HA	E	0.17092	0.17746
CC1	CA	B	−0.14998	−0.16565
HC1	HA	E	0.15434	0.16080
C121	CA	S	0.00463	0.03092
CC12	CA	B	−0.18392	−0.13924
HC12	HA	E	0.14358	0.14875
CC11	CA	B	−0.04200	−0.23532
HC11	HA	E	−0.00090	0.17144
C102	CA	S	−0.03802	0.01405
C101	CA	E	−0.09077	−0.05492
C3’	CT	M	0.07169	0.07157
H3’	H1	E	0.09904	0.09887
C2’	CT	B	−0.20223	−0.18867
H2’1	HC	E	0.08456	0.07930
H2’2	HC	E	0.08737	0.08783
O3’	OS	M	−0.52071	−0.52147

Table S2: Added Force Field Parameters

Angle	K_θ (kcal mol^{-1} rad^{-2})	θ_{eq} (deg)
N2–CT–CA	80.0	111.20
H1–CT–CA	50.0	109.50
OH–CT–CA	50.0	109.50

Table S3: Experimental (Cosman et al., 1992) and Trajectory Averaged Intermolecular NOE Derived Distances Involving BP Benzylic and Pyrenyl Rings for the 10*S* (+)-*trans-anti*-dG Adduct over Additional Different Time Frames

Experimental NOE				Range	1.5–2.0 ns	1.5–2.5 ns
HC11	G*6	H1′	G18	[2.76, 4.76]	4.41 (0.43)	4.39 (0.45)
HC9	G*6	H1′	C7	[2.03, 3.23]	2.40 (0.32)	2.36 (0.32)
HC10	G*6	H1′	C7	[2.81, 4.41]	4.38 (0.52)	4.34 (0.49)
HC2	G*6	H4′	A19	[2.94, 4.54]	3.15 (0.47)	3.15 (0.46)
HC9	G*6	H1′	G*6	[4.00, 6.00]	4.60 (0.50)	4.63 (0.47)
HC10	G*6	H1′	G*6	[2.85, 4.45]	3.83 (0.32)	3.77 (0.27)
HC10	G*6	HN	G*6	[2.50, 4.50]	2.97 (0.06)	2.97 (0.06)
HC8	G*6	HN	G*6	[2.00, 4.00]	2.37 (0.20)	2.38 (0.20)
HC9	G*6	HN	G*6	[3.00, 5.00]	3.23 (0.17)	3.22 (0.17)
HC8	G*6	H1	G*6	[2.68, 4.68]	3.90 (0.23)	3.92 (0.23)
HC9	G*6	H1	G*6	[3.53, 5.53]	4.52 (0.20)	4.53 (0.20)
HC8	G*6	H1	G16	[3.25, 5.25]	4.61 (0.56)	4.70 (0.53)
HC8	G*6	H1	G18	[3.30, 5.30]	7.28 (0.37)	7.33 (0.36)
HC4	G*6	H5′1	G18	[3.17, 5.17]	6.29 (0.69)	6.25 (0.74)
HC4	G*6	H5′2	G18	[3.17, 5.17]	6.69 (0.72)	6.67 (0.76)
HC5	G*6	H5′1	G18	[3.17, 5.17]	4.92 (0.47)	4.87 (0.53)
HC5	G*6	H5′2	G18	[3.17, 5.17]	4.80 (0.55)	4.78 (0.59)
HC6	G*6	H5′1	G18	[2.13, 4.13]	5.08 (0.42)	5.01 (0.48)
HC6	G*6	H5′2	G18	[2.13, 4.13]	4.15 (0.37)	4.10 (0.42)
HC4	G*6	H4′	G18	[2.31, 4.31]	4.41 (0.58)	4.41 (0.59)
HC4	G*6	H4′	A19	[2.31, 4.31]	4.16 (0.94)	4.21 (0.99)
HC5	G*6	H4′	G18	[2.31, 4.31]	2.91 (0.36)	2.91 (0.37)
HC5	G*6	H4′	A19	[2.31, 4.31]	5.87 (0.87)	5.91 (0.90)
HC1	G*6	H4′	A19	[2.69, 4.69]	4.09 (0.81)	4.07 (0.81)
HC3	G*6	H4′	A19	[2.69, 4.69]	2.98 (0.62)	3.02 (0.69)

Table S4: Experimental (de los Santos et al., 1992) and Trajectory Averaged Intermolecular NOE Derived Distances Involving BP Benzylic and Pyrenyl Rings for the 10R (−)-*trans-anti*-dG Adduct over Additional Different Time Frames

Experimental NOE				Range	1.5–2.0 ns	1.5–2.5 ns
HC9	G*6	H1	G*6	[2.68, 4.28]	4.83 (0.16)	4.85 (0.16)
HC9	G*6	HN	G*6	[2.20, 3.80]	3.64 (0.13)	3.65 (0.13)
HC10	G*6	HN	G*6	[1.96, 3.56]	2.72 (0.10)	2.72 (0.10)
HC10	G*6	H1′	G*6	[4.20, 5.70]	4.52 (0.35)	4.55 (0.33)
HC10	G*6	H1′	C7	[1.98, 3.38]	2.66 (0.42)	2.63 (0.41)
HC11	G*6	H1′	C7	[2.14, 3.14]	2.62 (0.41)	2.65 (0.40)
HC11	G*6	H4′	C7	[3.63, 5.13]	4.29 (0.60)	4.39 (0.59)
HC11	G*6	HN	G*6	[1.95, 3.55]	2.75 (0.23)	2.77 (0.23)
HC11	G*6	H1	G*6	[2.23, 3.83]	4.10 (0.28)	4.14 (0.28)
HC11	G*6	H1	G16	[2.85, 4.45]	4.71 (0.26)	4.69 (0.27)
HC12	G*6	H1′	C7	[3.18, 4.18]	4.04 (0.74)	4.10 (0.71)
HC12	G*6	H4′	T8	[1.91, 3.91]	3.21 (0.48)	3.20 (0.46)
HC12	G*6	HN	G*6	[2.51, 4.11]	4.66 (0.22)	4.69 (0.22)
HC12	G*6	H1	G*6	[2.84, 4.44]	5.59 (0.33)	5.65 (0.32)
HC12	G*6	H1	G16	[2.58, 4.18]	4.90 (0.38)	4.92 (0.36)
HC4	G*6	H4′	C17	[2.80, 4.40]	4.27 (0.57)	4.19 (0.57)
HC4	G*6	H4′	G18	[4.00, 5.50]	4.70 (0.59)	4.58 (0.59)
HC5	G*6	H4′	G18	[2.86, 3.86]	2.93 (0.42)	2.78 (0.44)
HC6	G*6	H1′	G18	[3.78, 5.28]	3.41 (0.41)	3.56 (0.47)
HC6	G*6	H4′	G18	[2.25, 3.25]	2.83 (0.37)	2.84 (0.35)
HC1	G*6	H1′	T8	[2.16, 3.16]	3.66 (0.62)	3.61 (0.58)
HC1	G*6	H4′	T8	[2.22, 3.22]	3.43 (0.69)	3.47 (0.70)
HC2	G*6	H1′	C17	[3.59, 5.09]	4.96 (0.35)	5.04 (0.35)
HC2	G*6	H1′	T8	[2.37, 3.37]	5.77 (0.70)	5.71 (0.67)
HC3	G*6	H4′	C17	[3.25, 4.75]	3.31 (0.40)	3.32 (0.39)
HC3	G*6	H1′	C17	[2.76, 4.36]	5.05 (0.35)	5.07 (0.34)

Table S5: Free Energy Analysis of the 10*S* (+)- and 10*R* (−)-*trans-anti*-dG Adducts over Additional Different Blocked and Windowed Time Frames

	1.5–2 ns	1.5–2.5 ns	1.5–3 ns (shifted 5 ps)
		10*S* (+)-*trans-anti*-dG adduct	
$\langle E_{\text{elec}} \rangle$	318.4 (44.1)	323.3 (45.4)	320.8 (43.4)
$\langle E_{\text{vdW}} \rangle$	−192.1 (10.3)	−192.1 (9.2)	−193.6 (10.2)
$\langle E_{\text{int}} \rangle$	1010.7 (22.3)	1013.4 (22.0)	1011.6 (21.6)
$\langle E_{\text{MM}} \rangle$	1137.0 (46.4)	1144.6 (45.9)	1138.9 (41.2)
$\langle G_{\text{nonpolar}} \rangle$	25.0 (0.2)	25.0 (0.2)	25.0 (0.2)
$\langle G_{\text{PB}} \rangle$	−5705.6 (37.7)	−5710.4 (39.3)	−5708.6 (40.7)
$\langle G_{\text{solvation}} \rangle$	−5680.5 (37.8)	−5685.4 (39.4)	−5683.6 (40.8)
$\langle G_{\text{PB}} + E_{\text{elec}} \rangle$	−5387.2 (12.5)	−5387.1 (12.6)	−5387.7 (11.9)
$\langle E_{\text{MM}} + G_{\text{PB}} \rangle$	−4568.6 (20.8)	−4565.8 (19.9)	−4569.7 (21.3)
$-TS$		−586.5	
G_{tot}	−5130.1	−5127.3	−5131.2
		10*R* (−)-*trans-anti*-dG adduct	
$\langle E_{\text{elec}} \rangle$	309.2 (44.3)	307.8 (40.9)	316.9 (42.6)
$\langle E_{\text{vdW}} \rangle$	−196.6 (8.9)	−196.5 (8.9)	−195.9 (10.5)
$\langle E_{\text{int}} \rangle$	1020.3 (18.8)	1017.0 (20.3)	1013.9 (20.4)
$\langle E_{\text{MM}} \rangle$	1132.9 (44.6)	1128.3 (40.0)	1134.9 (45.1)
$\langle G_{\text{nonpolar}} \rangle$	24.8 (0.2)	24.8 (0.2)	24.8 (0.2)
$\langle G_{\text{PB}} \rangle$	−5696.5 (43.1)	−5693.0 (37.7)	−5700.6 (40.7)
$\langle G_{\text{solvation}} \rangle$	−5671.7 (43.1)	−5668.2 (37.8)	−5675.8 (40.8)
$\langle G_{\text{PB}} + E_{\text{elec}} \rangle$	−5387.3 (11.8)	−5385.3 (12.2)	−5383.7 (11.3)
$\langle E_{\text{MM}} + G_{\text{PB}} \rangle$	−4563.6 (18.9)	−4564.7 (18.6)	−4565.7 (19.4)
$-TS$		−587.9	
G_{tot}	−5126.7	−5127.8	−5128.8
Δ	−3.4	0.5	−2.4

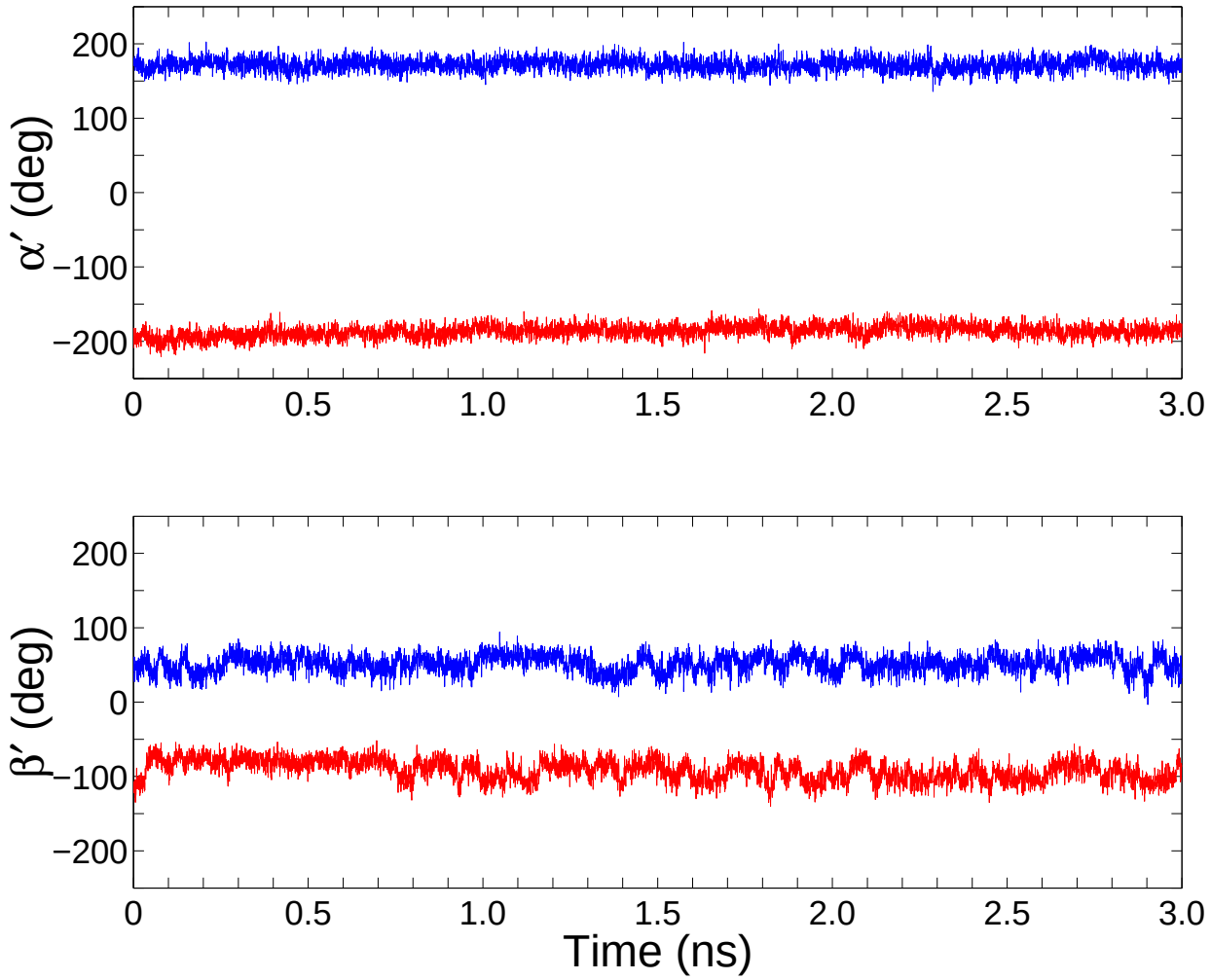

Figure S1: Torsion angles α' and β' for the 10*S* (+)-*trans-anti*-dG adduct (red) and 10*R* (−)-*trans-anti*-dG adduct (blue) over the 3-ns production MD simulation. Definitions of α' and β' are given in the caption to Figure 1.

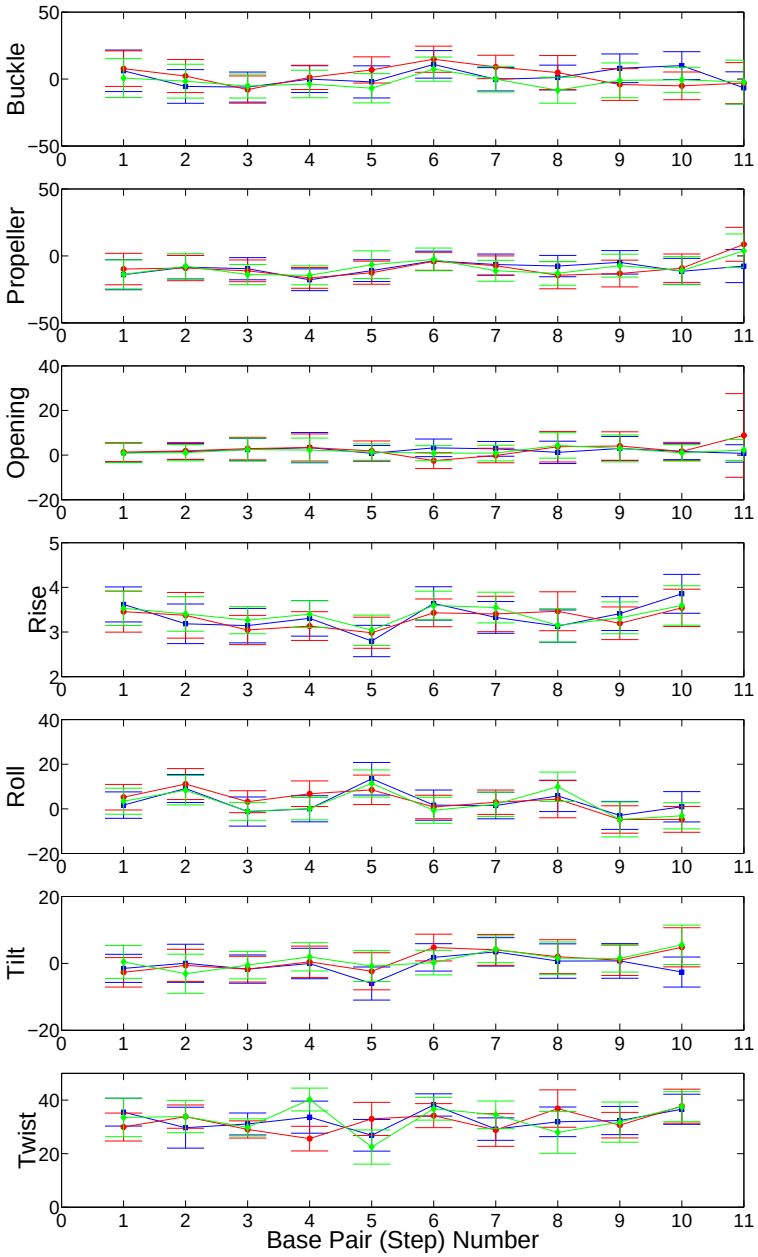

Figure S2: Average helicoidal parameters for the structures of the 10*S* (+)-*trans-anti*-dG adduct (red circles), 10*R* (−)-*trans-anti*-dG adduct (blue squares), and the unmodified control duplex (green diamonds) over 1.5–3 ns (3000 structures). The standard deviations are shown as error bars. The numbering scheme for the nucleotide base pair steps is that the C1–G22 to C2–G21 is step 1, the C2–G21 to A3–T20 is step 2, . . ., and so on. All values were calculated using Dials and Windows (Ravishanker et al., 1989).

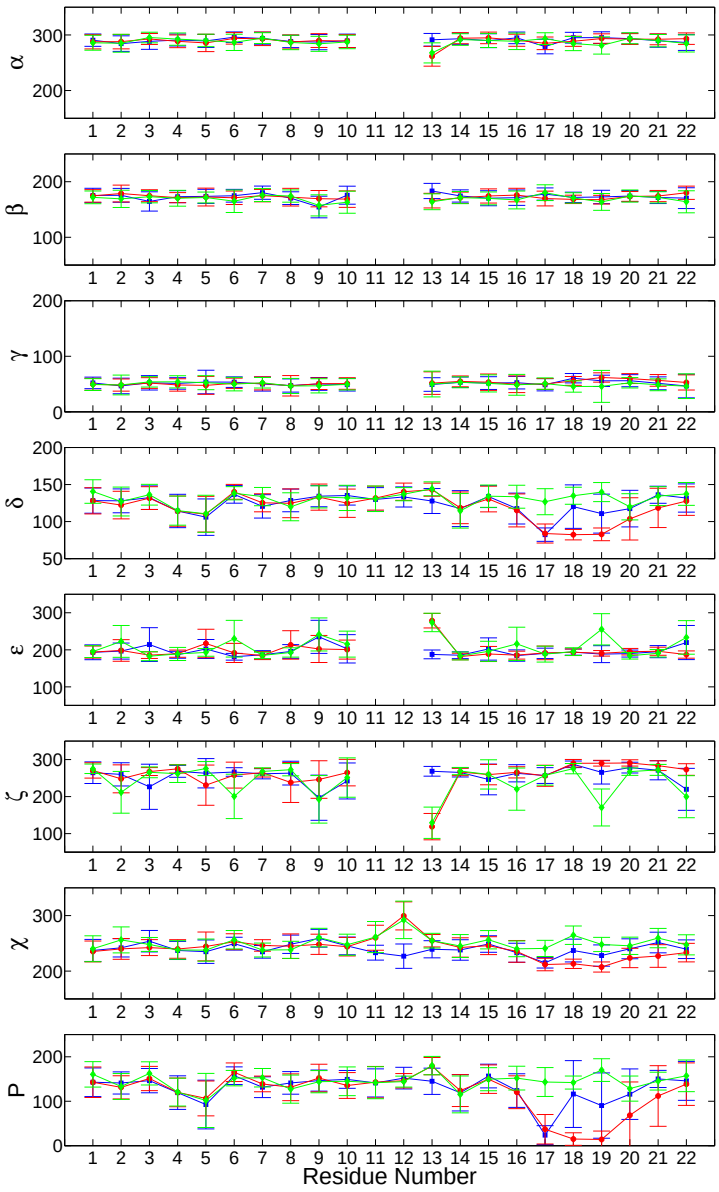

Figure S3: Average backbone torsional parameters for the structures of the 10*S* (+)-*trans-anti*-dG adduct (red circles), 10*R* (−)-*trans-anti*-dG adduct (blue squares), and the unmodified control duplex (green diamonds) over 1.5–3 ns (3000 structures). The standard deviations are shown as error bars. All values were calculated using Dials and Windows (Ravishanker et al., 1989). It should be noted that the residue numbers in Dials and Windows (Ravishanker et al., 1989) differ from the IUPAC convention (Saenger, 1984) as follows: For α, β, and γ, residue numbers 1–10 should be shifted +1, and for ϵ and ζ, residues 13–22 should be shifted −1 to accord with the IUPAC convention (Saenger, 1984).